Exp Brain Res (1999) 128:188–193

RESEARCH NOTE

Laetitia Gabernet · Virginia Meskenaïte
Marie-Claude Hepp-Reymond

Parcellation of the lateral premotor cortex of the macaque monkey based on staining with the neurofilament antibody SMI-32

Received: 30 October 1998 / Accepted: 4 March 1999

Abstract In macaque monkey, frontal and parasagittal brain sections were stained with SMI-32, an antibody directed against a nonphosphorylated neurofilament protein that labels pyramidal cells. The goal of this investigation was to find reliable criteria with which to draw the border between the motor (M1) and premotor (PM) cortex and delineate subdivisions within the lateral PM. Two-dimensional reconstruction of the staining patterns was also performed by flattening the series of frontal sections. The distribution of SMI-32 immunoreactivity in layers III and V of the cortex revealed the existence of three subregions in the ventral rostral PM and a clear mediolateral boundary within the dorsal PM defined by clusters of SMI-32-positive pyramidal cells in layer V. The border between M1 and PM was easily distinguished at the level of the dorsal PM by a strong loss of immunoreactive pyramidal cells in layers III and V. At the level of the ventral PM there was no clear disruption of layer V pattern, and the border was set using the pattern of layer III immunoreactivity.

Key words Lateral premotor cortex · SMI-32 · Pyramidal cell · Motor cortex · Primate

Introduction

The premotor cortex (PM) is functionally and architectonically heterogeneous and has been described in various ways (Brodmann 1909; Vogt and Vogt 1919; Bonin and Bailey 1947; Barbas and Pandya 1987). Patterns of cytochrome oxidase staining and cytoarchitectonics enabled Matelli et al. (1985, 1991) to subdivide the PM of the macaque monkey into six subareas. In the lateral PM they distinguished F4 (PM ventral caudal, PMvc), F5 (PM ventral rostral, PMvr), F2 (PM dorsal caudal, PMdc) and F7 (PM dorsal rostral, PMdr). Campbell and Morrison (1989), using a new antibody to nonphosphorylated neurofilament protein (SMI-32), demonstrated that a subpopulation of pyramidal cells was stained in the primate brain cortex. Recently, a series of investigations demonstrated that this immunoreactivity had specific regional distribution patterns. In the monkey this technique helped subdivide various brain regions, such as the superior temporal cortex, visual areas, orbital and medial prefrontal cortex and inferior pulvinar (Cusick et al. 1995; Chaudhuri et al. 1996; Hof and Morrison 1995; Carmichael and Price 1994; Gutierrez et al. 1995). Applying this technique to the monkey motor cortex (M1), Preuss et al. (1997) proposed three rostrocaudal subdivisions. SMI-32 was also processed in the human cortex for delineating regions within the orbitofrontal cortex (Hof et al. 1995) and the superior and mesial PM (Baleydier et al. 1997). The latter authors were able to easily define a caudal and a rostral subdivision in lateral area 6. They also stated that the SMI-32 staining was more reliable than cytochrome oxidase because of the extreme variations in this enzymic method.

In the present study we attempted to reinvestigate the controversial parcellation of the lateral PM with this new tool, which should be especially appropriate for demonstrating the various distribution of layer III and V pyramidal cells within the agranular frontal cortex.

Materials and methods

Two monkeys (*Macaca mulatta* and *M. fascicularis*) were given a lethal overdose of sodium pentobarbital, perfused transcardially with 0.4 l normal saline followed by 4 l fixative consisting of 4% paraformaldehyde in 0.1 M phosphate buffer pH at 7.4 (PB). Perfusion was continued with increasing concentration of sucrose up to 30% in PB. After the brain was removed from the skull, it was stored in cold 30% sucrose in PB as a cryoprotectant, prior to sectioning on a freezing microtome at 50 µm. Three hemispheres were cut in the coronal and one in the parasagittal plane. Every tenth section was processed for SMI-32 immunohistochemistry. A

L. Gabernet · M.-C. Hepp-Reymond
Brain Research Institute, University Zurich,
Zurich, Switzerland

L. Gabernet · V. Meskenaïte · M.-C. Hepp-Reymond (✉)
Institute of Neuroinformatics, University of Zurich-Irchel,
Winterthurerstrasse 190, CH-8057 Zurich, Switzerland,
e-mail: mchr@ini.phys.ethz.ch

series of adjacent sections were stained for Nissl bodies with cresyl violet, for cytochrome oxidase (CO), acetylcholinesterase (AChE), parvalbumin (PV), calretinin (CR), and the α1- and α2-subunits of the $GABA_A$ receptor.

The sections were preincubated in 20% normal goat serum in 0.05 M Tris-buffered saline at pH 7.4, which contained 0.5% Triton-X100 (TBST) for 60 min at room temperature. They were then incubated in SMI-32 monoclonal antibodies (1:7500, Sternberger Monoclonals Inc., MD) for 24–36 h at 4°C in TBST also containing 2% bovine serum albumin, 1% normal goat serum, and 2% normal monkey serum. Following 4×20-min washes in TBST, the sections were incubated for 12 h at 4°C in biotinylated secondary goat anti-mouse antibodies (1:200; Vector Laboratories, Burlingame, CA) and for 3 h in the Vectastain ABC Elite reagent (1:100, Vector Laboratories) at room temperature. Antigenic sites were visualized with standard 3,3'-diaminobenzidine tetrahydrochloride (DAB; Sigma, Switzerland) histochemistry. Firstly, sections were preincubated in 0.05% DAB in TB, pH 7.6, for 20–25 min. H_2O_2 was then added to the media to give a final concentration of 0.0048% and sections were incubated for a further 3–5 min. The reaction was stopped by several washes in TB. Sections were mounted on gelatinized slides from PB, air dried, dehydrated, and coverslipped in Entelan (E. Merck, Switzerland). As controls some adjacent sections were processed simultaneously as described above, except that the primary antibody was omitted or replaced by normal mouse serum.

SMI-32-labeled sections were examined under bright-field optics and compared with adjacent Nissl-stained sections. Sections were digitized under a camera driven by a multiple-channel imaging device system. Information from sections was compiled into a stack of digitized sections and the (10%) shrinkage due to perfusion (2%) and immunostaining (8%) was corrected. Flattened two-dimensional reconstructions of frontal cortex were produced for each hemisphere by "opening" the central (CS) and the arcuate (AS) sulcus on every section (adapted from Dum and Strick 1991). The portion of the cortex from the fundus of the AS and its caudal bank rostrally to the tip of the intraparietal sulcus caudally was reconstructed. Using this method the whole lateral PM and M1 cortex was flattened. SMI-32-labeled layer III was used as the reference layer since it was stained on the whole surface of the agranular frontal cortex. It was "straightened" mediolaterally from the hemispheric midline to the lateral sulcus on each frontal section. The boundaries within the PM were determined microscopically, marked on the printed digitized sections and projected to the straightened layer III. Every section was aligned on the midline (Fig. 3).

Results

Four hemispheres of two monkey brains were processed with the SMI-32 antibody. SMI-32 labeled a population of pyramidal cells in layers III and V. SMI-32-positive large pyramidal cells could be identified when compared with adjacent Nissl-stained sections. To set boundaries, several nonquantitative criteria were applied such as the density of layer III and discontinuities in the presence and number of layer V SMI-32-positive pyramidal cells. The boundary of labeled SMI-32-positive large pyramidal cells in layer V was the main criterion for drawing the border between M1 and PM. To set boundaries within PM the density of the staining in layer III assessed by visual observation was the main criterion.

Staining in the motor cortex

The staining in M1 and PM was quite strong compared with other adjacent cortical areas (Fig. 1F,G). Staining in M1 appeared at the level of the pyramidal cell bodies, and both apical and basal dendrites in layers III and V. M1 could be clearly characterized by its high number of SMI-32-positive pyramidal cells in layer V. Most of the Betz cells were labeled as could be judged from a comparison with the Nissl-stained sections. Layer III was also rich in immunoreactive pyramidal cells, which were generally smaller and less strongly stained than those observed in layer V. This layer was thick but not homogeneous in labeling. Some regions in M1, mainly in the rostral part, were stained less, for both layer III and layer V. In particular there was a disappearance of the immunoreactivity close to the CS crown (Figs. 1F, 2A). This decrease was observed in all four hemispheres processed.

Border between motor and premotor cortex

We distinguished the border between M1 and PM by the absence or strong decrease in the number of SMI-32-positive cells in layer V and by the decrease in immunoreactivity in layer III. The M1/PM border was obvious at the level of PMd (Figs. 1F, 2C,D, 3, left). PMd contained almost no labeled cells in layer V and only a low density of SMI-32-positive cells in layer III. However, several clusters of SMI-32-positive cells in layer V were found in the superior precentral sulcus (SPcS) and more rostrally (Fig. 1E,F). These cell clusters can be used to define a mediolateral partition within PMd (Fig. 3: 3 vs 8 and 2) as the cortex in the medial direction contained a thinner layer III and had weaker staining than in its lateral aspect.

The border of M1 with PMv is less clear than it is with PMd due to the presence of many immunoreactive pyramidal cells in layer V in PMvc. At this level, SMI-32-positive pyramidal cells in layer V showed no discontinuity from caudal to rostral and made it difficult to delineate an M1/PM border on the single criterion of layer-V-labeled cells. However, this border could be set taking as criteria both the strong decrease in density and size of the layer V pyramidal cells and the thinner and less dense layer III (Fig. 2A,B).

Borders within PM

The distribution of layer V SMI-32-positive pyramidal cells in PMv was a useful feature with which to draw the limit between PMv and PMd. In PMd, layer V was poorly labeled or mostly absent (Figs. 1E, 2C) except for the region close to the spur. Within PMd two subdivisions could also be distinguished in the rostrocaudal direction: a caudal region containing SMI-32-positive cell clusters (PMdc) and a quite rostral region showing very poor immunoreactivity (PMdr). In Figs. 2C,D and 3, these subregions are numbered 2 and 8 respectively.

PMvr and PMvc can also be distinguished on the basis of the SMI-32 staining, the border being defined by the strong decrease in the density of the layer III staining (Fig.

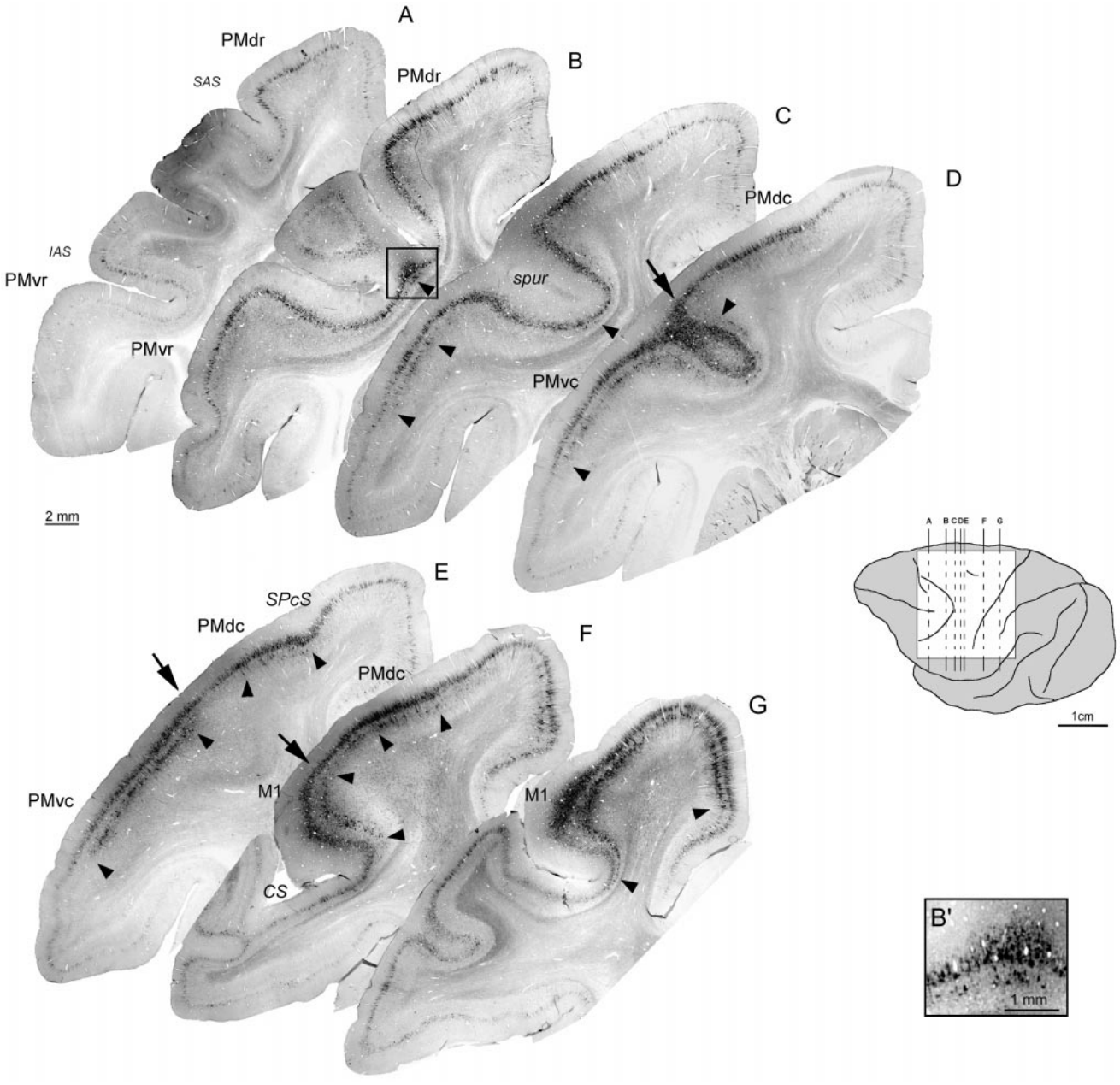

Fig. 1A–G SMI-32 staining in a series of frontal sections through the monkey agranular frontal cortex (*Macaca mulatta*). Pyramidal cells in layers V and III are labeled. SMI-32 immunoreactivity shows distinct labeling patterns in the primary motor (*M1*) and premotor (*PM*) areas. *On the right* is a sketch showing the location of the sections from rostral **(A)** to caudal **(G)** (same hemisphere as Fig. 3, left). *Arrows* indicate boundaries set according to the presence and the density of labeled pyramidal cells in layers III and V between: *PMvr* (PM ventral rostral), *PMvc* (PM ventral caudal), *PMdr* (PM dorsal rostral), *PMdc* (PM dorsal caudal) and the border between *PMdc* and *M1*. *Arrowheads* indicate the presence of layer V SMI-32-positive cells (*IAS* inferior arcuate sulcus, *SAS* superior arcuate sulcus, *CS* central sulcus, *SPcS* superior precentral sulcus). *Inset* **(B')** enlargement of the spur region in section B showing scattered large pyramidal cells in layer V

2A,B). PMvr (F5) was generally weakly stained, without any layer V SMI-32-positive cells, except in a region close to the spur. Parasagittal sections allowed us to define more clearly three PMvr subdivisions labeled 7, 6 and 5 in Fig. 2A–C. Firstly, the most rostral and lateral region (7) showed almost no SMI-32 staining, except some pale processes in layer III. An adjacent caudal part (6) contained a thin weak but clear SMI-32-positive layer III. The third subdivision (spur region, 5) had a thick and highly immunoreactive layer III and contained scattered large pyramidal cells in layer V (Fig. 1B–D and inset B'). These large SMI-32-positive layer V neurons around the spur are also visible in the sagittal sections of Fig. 2.

To obtain a precise and clear overview of the staining pattern within the AS, we opened the sulcus by flattening the series of frontal sections and reconstructing

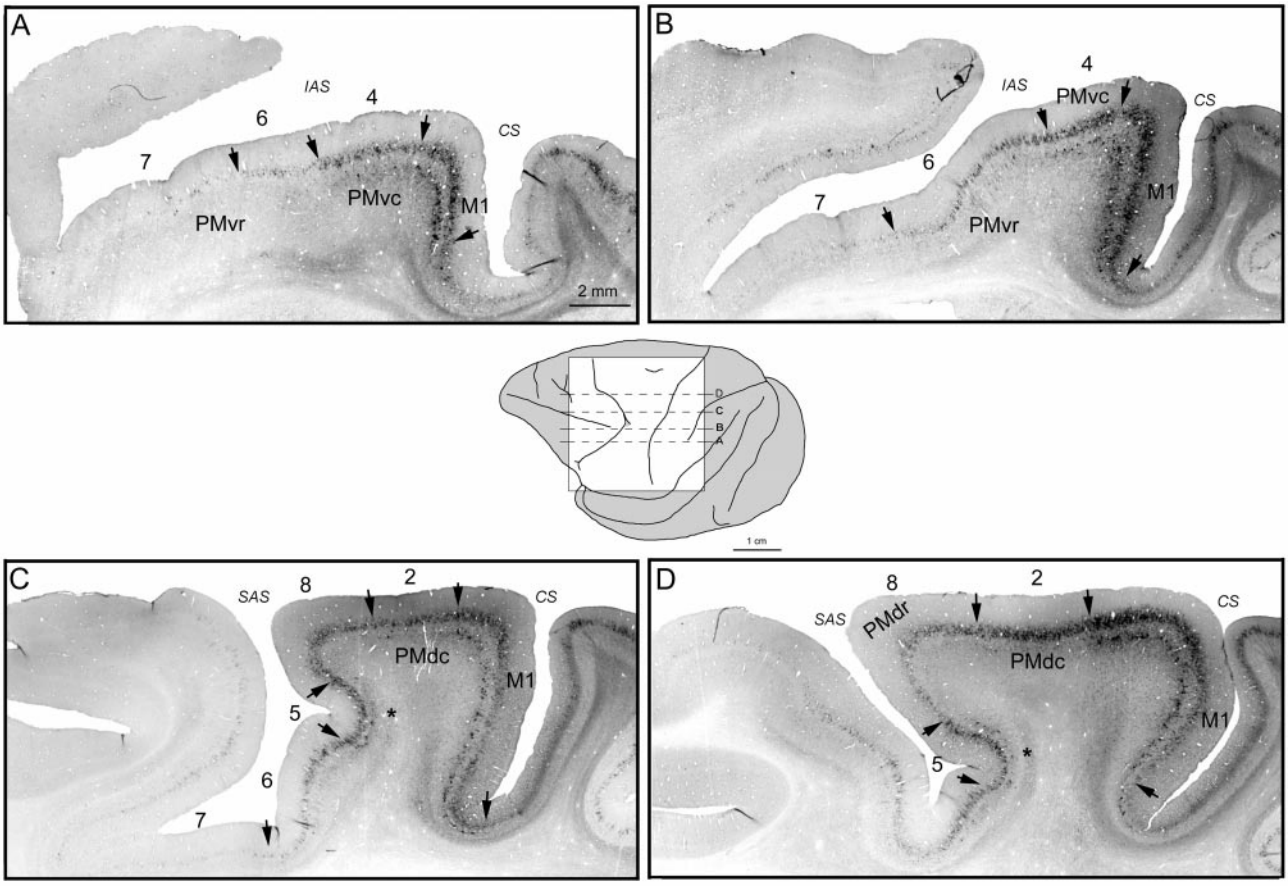

Fig. 2A–D SMI-32 staining in a selection of parasagittal sections through the monkey frontal cortex (*Macaca mulatta*). *Center* sketch of the left hemisphere showing the location of the sections from ventral **(A)** to dorsal **(D)**. *Arrows* indicate boundaries within the lateral PM and between PM and M1 according to the criteria described in Fig. 1. *Numbers* correspond to the parcellation of the lateral PM shown in the sketches in Fig. 3 and discussed in the text (*2* PMdc, *4* PMvc, *5* PMvr spur, *6* PMvr intermediate, *7* PMvr rostral, *8* PMdr). *Stars* indicate layer V pyramidal cells in PMdr, close to the AS internal spur. For abbrevations see Fig. 1

the surface of the stained cortex. The opening of the CS and AS created distortions on the reconstructed maps at the level of the AS spur and the CS foot, which can be appreciated as strong irregularities in the course of the lateral sulcus (Fig. 3). These flattened reconstructions revealed the subdivisions within PMvr, and the various possible boundaries in PMd. They also allowed a comparison between animals and hemispheres. These maps clearly show the continuous presence of layer V pyramidal cells from the CS to the AS at the level of the spur. They are still preliminary as they do not include the rostrocaudal gradient in density and size of the SMI-32-stained pyramidal cells, which was used to draw the line between M1 and PMvc. In the drawings representing the lateral surface of the two flattened brains, an attempt has been made to trace the borders and show the parcellation of PM discussed in the text. Unfortunately this representation is incomplete on this surface view of the brain, as some borders are located within the sulci and therefore cannot be represented on a surface map.

Discussion

The distribution of neurofilament protein with SMI-32 antibody displayed different patterns of immunoreactivity within the agranular frontal cortex. On the basis of the immunoreactivity in layer III and V pyramidal cells, we were able to set a clear border between M1 and PM, even at the level of PMvc, which still contains SMI-32-positive pyramidal cells. Boundaries in this very region have often not been easy to define, although Matelli et al. (1985) found some criteria with which to set their F1/F4 border on the basis of CO staining. Our M1/PM borders, which are supported by adjacent sections stained for CO, AchE and Nissl (Gabernet et al. 1997), seem to correspond with the ones proposed by Matelli et al. (1985). In addition, striking differences between the immunoreactive patterns of PMd as compared to PMv were obvious mainly on the frontal sections. In PMd we also found a clear mediolateral boundary defined by the clusters of SMI-32-positive pyramidal cells in layer V at the level of the SPcS and more rostrally. Although the poor immunoreactivity in the most dorsal PMd could be attributed in Fig. 1 to inhomogeneity in the section thickness, we do not think that it is the case as similar gradients have been clearly observed in two other hemi-

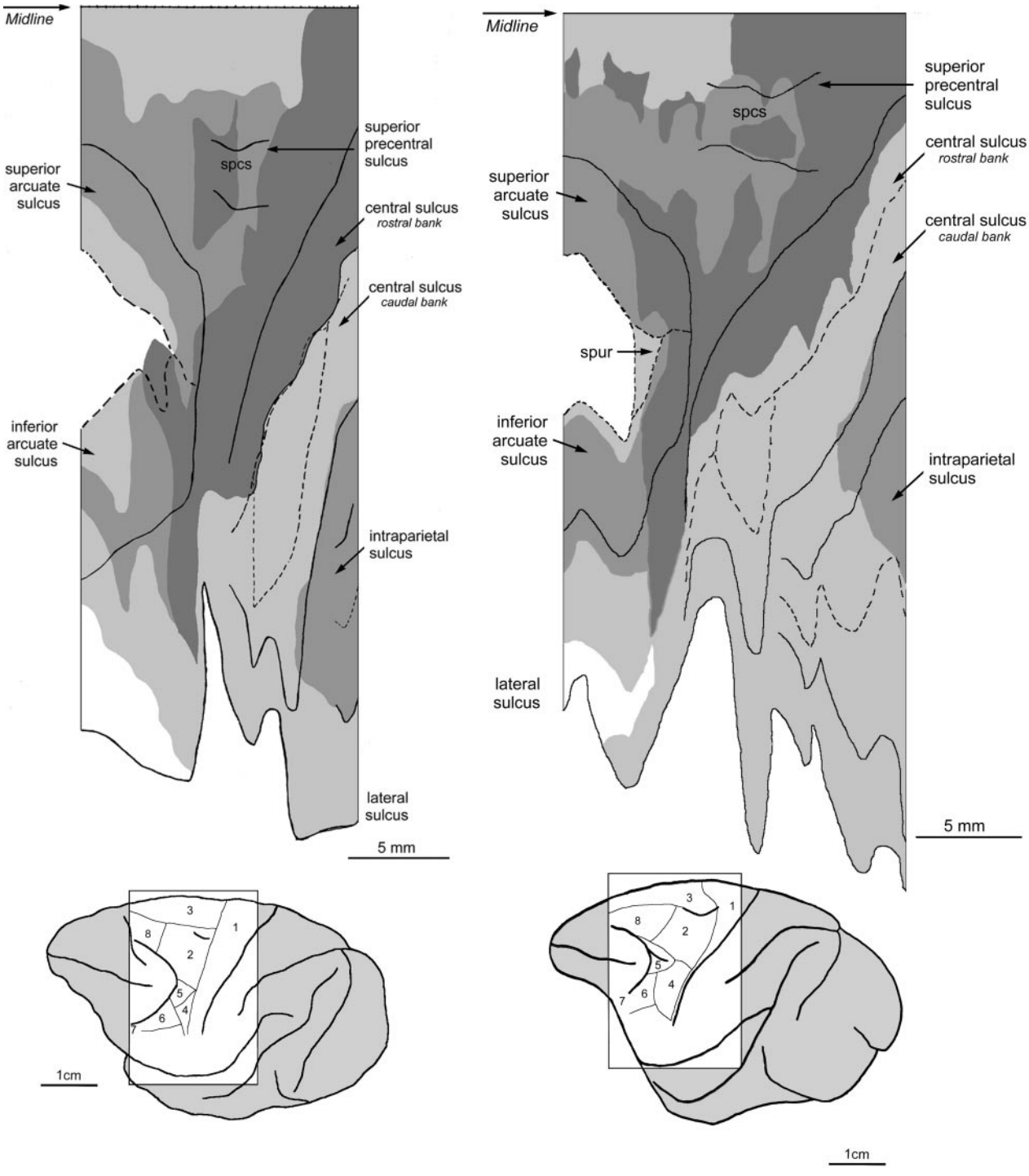

Fig. 3 *Top* Flattened reconstructions of SMI-32-staining patterns in two monkeys (*left M. mulatta*, same as Fig. 1; *right M. fascicularis*). Flattened sections aligned on the midline (junction of the medial wall with the lateral surface of the cortex) [*dashed lines* fundus of each opened sulcus, *full lines* crowns of sulci, except for the most caudal line of AS which marks the end of the internal spur (section displayed in Fig. 1D), *dark gray* region of the cortex with dense-labeled layer III and layer V pyramidal cells, *middle gray* cortical regions with labeled layer III only, *pale gray* portions of PM with weak staining in layer III]. *Bottom* Lateral view of the corresponding brains with a drawing of the subdivisions discussed in the text (*1* M1, *2* PMdc, *3* PMd medial, *4* PMvc, *5* PMvr spur, *6* PMvr intermediate, *7* PMvr rostral, *8* Pmdr)

spheres (Fig. 3). A mediolateral partition of PMd has also been suggested on the basis of SMI-32 immunoreactivity by Geyer et al. (1998).

Rostrocaudal subdivisions within PMd (8, 2) could be best seen on parasagittal sections and may correspond to the F2 and F7 of Matelli et al. (1991). The caudal region with cell clusters in the SPcS was defined as belonging to PMdc. Preuss et al. (1997), because of the presence of layer V pyramidal cells, decided that this region still belonged to M1 as a third rostral region (4r). As can be clearly seen in Fig. 3, discontinuities in layer V SMI-32

labeling between the CS and the SPcS strongly suggest that this region is not an extension of M1 but rather belongs to PMd. In fact, we showed in two monkeys that low-current intracortical microstimulation (ICMS) elicited finger movements in the region of the clusters, revealing a new PM finger region localized more rostrally and separate from the caudal M1 hand representation (Qi et al. 1994). Our localization of the M1/PMd border agrees with the generally accepted one (He et al. 1993).

In PMv, although the boundary between rostral and caudal regions (F4/F5) was not sharp everywhere, subdivisions could be distinguished. PMvc was defined as having a staining pattern rather similar to that of M1, but with less numerous cells in layer V and a fainter layer III. This part of the PMv could not be additionally subdivided mediolaterally as reported by Geyer et al. (1998). An interesting finding is that the PMvr (F5) could be subdivided into three parts, as previously suggested by Matelli et al. (1996) on the basis of various stainings. The most rostral and lateral one was without any SMI-32 immunoreactivity but with a semigranular layer IV and particularly well laminated staining patterns in adjacent sections stained for AChE, PV, CR, CO and α1- and α2-subunits of the $GABA_A$ receptor (Fig. 3: 7). A caudal adjacent one had a weak SMI-32 immunoreactivity in layer III, and the most caudal and medial region at the level of the spur contained striking immunoreactivity in layer V (Fig. 3: 6 and 5 respectively). This small region can be compared with the region found in the fundus of the SPcS and looks like an island of scattered immunoreactive layer V pyramidal cells, similar but independent of M1 proper. This point is corroborated by functional data showing that within the arcuate spur, and also lateral to it, ICMS could elicit finger movements, even at relatively low currents (Hepp-Reymond et al. 1994; Gabernet et al. 1997). For one of the hemispheres processed in the present study, the ICMS sites have also been reconstructed on a flattened map that could be compared with the anatomical one. We found that the PM sites with the lowest current threshold for eliciting finger movements could in part be superimposed on the islands of SMI-32-positive pyramidal cells (unpublished data). These islands could also correspond to clusters of corticospinal neurons described by Dum and Strick (1991) and He et al. (1993).

In conclusion, the distribution of SMI-32 is a useful tool with which to parcellate the M1 and PM areas. Although the lateral PM cortex can be quite variable from monkey to monkey at the macroscopic and microscopic levels, some general features could be assessed to define various anatomical subdivisions within this region.

Acknowledgements This study was supported by the Swiss National Research Foundation, grant no. 31-39679.93, the National Research Program 38, grant no. 40-52837/1, and the Schweizerische Hochschulrektorenkonferenz. We thank Dr. P. Streit for help with the MCID system, Dr. A. McKinney for critically reading the manuscript and D. Latawiec for expert technical assistance.

References

Baleydier C, Achache P, Froment JC (1997) Neurofilament architecture of superior and mesial premotor cortex in the human brain. Neuroreport 8:1691–1696

Barbas H, Pandya DN (1987) Architecture and frontal cortical connections of the premotor cortex (area 6) in the rhesus monkey. J Comp Neurol 256:211–228

Bonin G von, Bailey P (1947) The neocortex of *Macaca mulatta*. University of Illinois Press, Urbana, IL

Brodmann K (1909) Vergleichende Localizationslehre der Grosshirnrhinde in ihren Prinzipien dargestellt auf Grund des Zellenbaues. Barth, Leipzig

Campbell MJ, Morrison JH (1989) Monoclonal antibody to neurofilament protein (SMI-32) labels a subpopulation of pyramidal neurons in the human and monkey neocortex. J Comp Neurol 282:191–205

Carmichael ST, Price JL (1994) Architectonic subdivision of the orbital and medial prefrontal cortex in the macaque monkey. J Comp Neurol 346:366–402

Chaudhuri A, Zangenehpour S, Matsubara JA, Cynader MS (1996) Differential expression of neurofilament protein in the visual system of the vervet monkey. Brain Res 709:17–26

Cusick CG, Seltzer B, Cola M, Griggs E (1995) Chemoarchitectonics and corticocortical terminations within the superior temporal sulcus of the rhesus monkey: evidence for subdivisions of superior temporal polysensory cortex. J Comp Neurol 360:513–535

Dum RP, Strick PL (1991) The origin of corticospinal projections from the premotor areas in the frontal lobe. J Neurosci 11:667–689

Gabernet L, Qi H-X, Arnold M, Hepp-Reymond M-C (1997) Subdivisions in the lateral premotor cortex revealed by various anatomical criteria and functional correlates. Soc Neurosci Abstr 23:1274

Geyer S, Matelli M, Luppino G, Zilles K (1998) A new microstructural map of the macaque monkey lateral premotor cortex based on neurofilament protein distribution. EJN 10 Suppl 10:83

Gutierrez C, Yaun A, Cusick CG (1995) Neurochemical subdivisions of the inferior pulvinar in macaque monkeys. J Comp Neurol 363:545–562

He SQ, Dum RP, Strick PL (1993) Topographic organization of corticospinal projections from the frontal lobe: motor areas on the lateral surface of the hemisphere. J Neurosci 13:952–980

Hepp-Reymond M-C, Hüsler EJ, Maier MA, Qi H-X (1994) Force-related neuronal activity in two regions of the primate ventral premotor cortex. Can J Physiol Pharmacol 72:571–579

Hof PR, Morrison JH (1995) Neurofilament protein defines regional patterns of cortical organization in the macaque monkey visual system: a quantitative immunohistochemical analysis. J Comp Neurol 352:161–186

Hof PR, Mufson EJ, Morrison JH (1995) Human orbitofrontal cortex: cytoarchitecture and quantitative immunohistochemical parcellation. J Comp Neurol 359:48–68

Matelli M, Luppino G, Rizzolati G (1985) Patterns of cytochrome oxidase activity in the frontal agranular cortex of the macaque monkey. Beh Brain Res 18:125–136

Matelli M, Luppino G, Rizzolati G (1991) Architecture of superior and mesial area 6 and the adjacent cingulate cortex in the macaque monkey. J Comp Neurol 311:445–462

Matelli M, Luppino G, Govoni P, Geyer S (1996) Anatomical and functional subdivisions of inferior area 6 in macaque monkey. Soc Neurosci Abstr 22:2024

Preuss TM, Stepniewska I, Jain N, Kaas JH (1997) Multiple divisions of macaque precentral motor cortex identified with neurofilament antibody SMI-32. Brain Res 767:148–153

Qi H-X, Hüsler EJ, Alig I, Hepp-Reymond M-C (1994) Simple and complex relations of cortical activity in the alert monkey. Soc Neurosci Abstr 20:60

Vogt O, Vogt C (1919) Allgemeine Ergebnisse unserer Hirnforschung. J Psychol Neurol (Leipzig) 25:277–462